Nonlinear dissipation-induced photon blockade

Xin Su (苏欣) [1,2] Jiang-Shan Tang (唐江山) [1,3,*] and Keyu Xia (夏可宇) [1,†]

[1]*College of Engineering and Applied Sciences, and National Laboratory of Solid State Microstructures, Nanjing University, Nanjing 210093, China*
[2]*School of Electronic Science and Engineering, Nanjing University, Nanjing 210093, China*
[3]*School of Physics, Nanjing University, Nanjing 210023, China*

We propose a theoretical scheme for photon blockade in a cavity quantum electrodynamic system consisting of an N-type atomic medium interacting with a single-mode Fabry-Pérot cavity. In contrast to inefficient nonlinear-dispersion-induced photon blockade suppressed by a large detuning of atomic transitions, the photon blockade in our scheme is induced by a large nonlinear dissipation of the cavity created by the near-resonant N-type atomic system. A deep photon blockade is manifested by a vanishing equal-time second-order correlation function within the cavity linewidth. We also provide an explanation for this dissipation-induced photon blockade. This work provides an efficient photon blockade because it works in the near-resonance case.

I. INTRODUCTION

Manipulation of single photons has been one of the key tasks of quantum information science and technology. It can be linear operation on photons, such as the storage and state manipulation of photons [1–7], or nonlinear operations, such as the generation of single photons via photon blockade (PB) [8–11] and quantum logic gates [12–17]. The nonlinear control of photons requires strong photon-excitation interaction [18–21], or conventionally a giant dispersive Kerr nonlinearity [22–26], in which the phase of a signal field is modified by an amount proportional to the photon number in another field or its own photon number, with both of the two fields containing few photons. The giant optical Kerr nonlinearity promises a great number of important applications such as nondestructive measurement of photons [27–30], generation of photonic chirality [31,32], single-photon switches, and transistors [33–37]. Moreover, it also attracts intense research because it can be utilized to prepare single photons via the PB effect. The giant Kerr nonlinearity in an optical cavity can cause energy anharmonicity to different photonic Fock states. Thus, absorption of a first photon introduces a large detuning to the cavity mode and thus blocks the successive excitation of higher Fock states. This PB effect therefore only allows the single-photon state to transmit the system and probabilistically generate a single-photon field.

However, the dispersive Kerr nonlinearity of optical materials is typically negligible at the single-photon level [38]. To tackle this problem, various quantum nonlinear systems such as atom-cavity systems [8,23], Rydberg atomic ensembles [39,40], and single quantum dots strongly coupling to a photonic crystal cavity [41,42] have been proposed to generate a strong PB effect. Among these systems, a cavity quantum electrodynamics system embedded with an N-type atomic system has been proposed theoretically [22–25,43] and demonstrated experimentally [44–47] to induce a giant Kerr nonlinearity with vanishing one-photon absorption. This absorptive-free giant Kerr nonlinearity promises significant practical applications for the PB effect [23,45,48,49]. Nevertheless, it is suppressed by a large detuning in the case of nonresonance, in order to dominate the two-photon absorption. As a result, the efficiency of the PB induced by this dispersive nonlinearity is limited. However, in comparison with the dispersive Kerr nonlinearity, a larger two-photon absorption [50–54] can be obtained with the N-type atomic system in the resonant case, giving rise to a stronger PB effect.

The capability of observing antibunching photons via multiphoton absorption processes has been discussed in previous works but very mathematically [50,51,55–57]. In this paper we show a strong PB by virtue of the two-photon absorption of an optical cavity induced by the N-type atomic ensemble. In the conventional PB caused by a dispersive Kerr nonlinearity in the N-type system, the Kerr nonlinearity is suppressed by a large detuning of atomic transitions. In contrast, the dissipative nonlinearity in our scheme is obtained in the atomic resonance case and thus greatly enhanced. We also provide a transparent physical picture for understanding this PB effect induced by nonlinear dissipation. Our scheme paves the way for using nonlinear dissipation as an alternative mechanism for the PB, which can be used to efficiently extract single photons from a weak coherent state of light.

Our paper is organized as follows. In Sec. II we describe our system and the model and use the perturbation method to analyze the effect of the N-type system on the Fabry-Pérot cavity: one-photon absorption, dispersion, and two-photon nonlinearity. In Sec. III we explain the mechanism of the PB induced by the two-photon absorption. In Sec. IV we show the results for nonlinear dissipation-induced PB and the

---

*js.tang@nju.edu.cn
†keyu.xia@nju.edu.cn
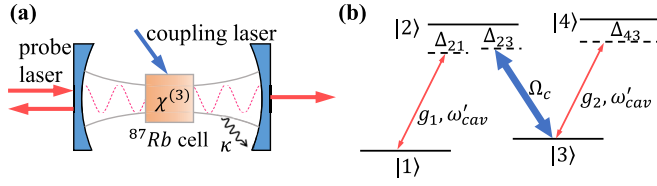
FIG. 1. (a) Schematic diagram of our system. A cell with an ensemble of ^{87}Rb atoms is placed in the cavity. (b) Related level structure of ^{87}Rb atoms.

transmission. In Sec. V we present the experimental implementation for our proposal. We conclude our work in Sec. VI with a brief discussion and summary.

II. SYSTEM AND MODEL

Our system for PB is schematically shown in Fig. 1(a). It consists of a Fabry-Pérot (FP) cavity and an ensemble of ^{87}Rb atoms. The related level structure of the ^{87}Rb atoms is depicted in Fig. 1(b). The atom in the N-type configuration has two ground states denoted by $|1\rangle$ and $|3\rangle$ and two excited states denoted by $|2\rangle$ and $|4\rangle$. A strong-coupling laser with frequency ω_c is applied to the $|3\rangle \leftrightarrow |2\rangle$ transition. The $|1\rangle \leftrightarrow |2\rangle$ and $|3\rangle \leftrightarrow |4\rangle$ transitions are coupled to the cavity mode simultaneously. A weak probe laser with frequency ω_p drives the cavity via the input mirror with rate κ_{e1}. The cavity field escapes from the output mirror with rate κ_{e2}. We assume that the intrinsic decay rate of the cavity is κ_i. It is negligible in our system. For simplicity, we set $\kappa_{e1} = \kappa_{e2}$. Thus, the cavity field decays at a total rate of $\kappa = \kappa_{e1} + \kappa_{e2} + \kappa_i$.

The Hamiltonian of the system in the rotating frame takes the form

$$
\hat{H} = -\Delta \hat{a}^\dagger \hat{a} + \sum_{j=1}^{N} \Big[\Delta_{21} \hat{\sigma}_{22}^j + (\Delta_{21} - \Delta_{23}) \hat{\sigma}_{33}^j
$$
$$
+ (\Delta_{21} - \Delta_{23} + \Delta_{43}) \hat{\sigma}_{44}^j + ig_1 \big(\hat{a}^\dagger \hat{\sigma}_{12}^j - \hat{\sigma}_{21}^j \hat{a} \big)
$$
$$
+ ig_2 \big(\hat{a}^\dagger \hat{\sigma}_{34}^j - \hat{\sigma}_{43}^j \hat{a} \big) + i \big(\Omega_c^* \hat{\sigma}_{32}^j - \Omega_c \hat{\sigma}_{23}^j \big) \Big]
$$
$$
+ i\sqrt{\kappa_{e1}} \varepsilon_p (\hat{a}^\dagger - \hat{a}). \tag{1}
$$

The first term in Eq. (1) is the free Hamiltonian of the intracavity field with annihilation and creation operators $\hat{a}$ and $\hat{a}^\dagger$, respectively, with $\Delta = \omega_p - \omega_{cav}$ the detuning between the probe field and the bare cavity resonance. The first three terms in square brackets represent the internal energy of the jth atom with $\hat{\sigma}_{mn}^j \equiv |m_j\rangle\langle n_j|$ ($m, n = 1, 2, 3, 4$) being the population operators (for $m = n$) or the atomic raising and lowering operators (for $m \neq n$) of the jth atom, in which $\Delta_{21} = \omega_{21} - \omega_{cav} - \Delta$ and $\Delta_{43} = \omega_{43} - \omega_{cav} - \Delta$ are the detunings between the corresponding transitions and the probe field and $\Delta_{23} = \omega_{23} - \omega_c$ is the detuning between the $|3\rangle \leftrightarrow |2\rangle$ transition and the coupling laser. The fourth (fifth) term in square brackets describes the coupling between the cavity mode and the $|1\rangle \leftrightarrow |2\rangle$ ($|3\rangle \leftrightarrow |4\rangle$) transition with the coupling rate g_1 (g_2). The last term in square brackets expresses the interaction between the coupling laser and the $|3\rangle \leftrightarrow |2\rangle$ transition, in which $\Omega_c = \mu_{23} E_c / 2\hbar$ is the half Rabi frequency of the coupling laser. The last term describes the coupling

between the monochromatic continuous-wave probe field and the cavity mode, the amplitude of the probe field being $\varepsilon_p = \sqrt{P/\hbar\omega_p}$, where P is the input power.

The decay and dephasing of the system can be described by the Lindblad operator

$$
\hat{\mathcal{L}}\hat{o} = \frac{\kappa}{2} [2\hat{a}^\dagger \hat{o}\hat{a} - \hat{a}^\dagger \hat{a}\hat{o} - \hat{o}\hat{a}^\dagger \hat{a}]
$$
$$
+ \frac{\gamma_{nm}}{2} \sum_{j=1}^{N} \big[2\hat{\sigma}_{nm}^j \hat{o}\hat{\sigma}_{mn}^j - \hat{\sigma}_{nn}^j \hat{o} - \hat{o}\hat{\sigma}_{nn}^j \big], \tag{2}
$$

where $\gamma_{nm} = \{\Gamma_{41}, \Gamma_{43}, \Gamma_{42}, \Gamma_{21}, \Gamma_{23}, \Gamma_{31}\}$, with Γ_{nm} denoting the spontaneous decay or dephasing rates from the state $|n_j\rangle$ to the state $|m_j\rangle$ and $\hat{\sigma}_{mn} = \{\hat{\sigma}_{14}, \hat{\sigma}_{34}, \hat{\sigma}_{24}, \hat{\sigma}_{12}, \hat{\sigma}_{32}, \hat{\sigma}_{13}\}$. Incorporating the Lindblad operator into the Heisenberg's equations derived from Eq. (1), the evolution of the system is given by the quantum Langevin equations

$$
\dot{\hat{a}} = \left(i\Delta - \frac{\kappa}{2} \right) \hat{a} + g_1 \sum_{j=1}^{N} \hat{\sigma}_{12}^j + g_2 \sum_{j=1}^{N} \hat{\sigma}_{34}^j + \sqrt{\kappa_{e1}} \varepsilon_p,
$$
$$
\tag{3a}
$$

$$
\dot{\hat{\sigma}}_{11}^j = \Gamma_{31}\hat{\sigma}_{33}^j + \Gamma_{21}\hat{\sigma}_{22}^j + \Gamma_{41}\hat{\sigma}_{44}^j + g_1\big(\hat{a}^\dagger\hat{\sigma}_{12}^j + \hat{\sigma}_{21}^j\hat{a}\big),
$$
$$
\tag{3b}
$$

$$
\dot{\hat{\sigma}}_{22}^j = -(\Gamma_{21} + \Gamma_{23})\hat{\sigma}_{22}^j + \Gamma_{42}\hat{\sigma}_{44}^j - \big(\Omega_c^*\hat{\sigma}_{32}^j + \Omega_c\hat{\sigma}_{23}^j\big)
$$
$$
- g_1\big(\hat{a}^\dagger\hat{\sigma}_{12}^j + \hat{\sigma}_{21}^j\hat{a}\big), \tag{3c}
$$

$$
\dot{\hat{\sigma}}_{33}^j = -\Gamma_{31}\hat{\sigma}_{33}^j + \Gamma_{23}\hat{\sigma}_{22}^j + \Gamma_{43}\hat{\sigma}_{44}^j + \big(\Omega_c^*\hat{\sigma}_{32}^j + \Omega_c\hat{\sigma}_{23}^j\big)
$$
$$
+ g_2\big(\hat{a}^\dagger\hat{\sigma}_{34}^j + \hat{\sigma}_{43}^j\hat{a}\big), \tag{3d}
$$

$$
\dot{\hat{\sigma}}_{44}^j = -(\Gamma_{42} + \Gamma_{43} + \Gamma_{41})\hat{\sigma}_{44}^j - g_2\big(\hat{a}^\dagger\hat{\sigma}_{34}^j + \hat{\sigma}_{43}^j\hat{a}\big), \tag{3e}
$$

$$
\dot{\hat{\sigma}}_{23}^j = -\tilde{\gamma}_{23}\hat{\sigma}_{23}^j - \Omega_c^*\big(\hat{\sigma}_{33}^j - \hat{\sigma}_{22}^j\big) - g_1\hat{a}^\dagger\hat{\sigma}_{13}^j + g_2\hat{a}^\dagger\hat{\sigma}_{24}^j,
$$
$$
\tag{3f}
$$

$$
\dot{\hat{\sigma}}_{14}^j = -\tilde{\gamma}_{14}\hat{\sigma}_{14}^j + g_1\hat{\sigma}_{24}^j\hat{a} - g_2\hat{\sigma}_{13}^j\hat{a}, \tag{3g}
$$

$$
\dot{\hat{\sigma}}_{12}^j = -\tilde{\gamma}_{12}\hat{\sigma}_{12}^j - \Omega_c\hat{\sigma}_{13}^j - g_1\big(\hat{\sigma}_{11}^j - \hat{\sigma}_{22}^j\big)\hat{a}, \tag{3h}
$$

$$
\dot{\hat{\sigma}}_{13}^j = -\tilde{\gamma}_{13}\hat{\sigma}_{13}^j + \Omega_c^*\hat{\sigma}_{12}^j + g_1\hat{\sigma}_{23}^j\hat{a} + g_2\hat{a}^\dagger\hat{\sigma}_{14}^j, \tag{3i}
$$

$$
\dot{\hat{\sigma}}_{24}^j = -\tilde{\gamma}_{24}\hat{\sigma}_{24}^j - \Omega_c^*\hat{\sigma}_{34}^j - g_1\hat{a}^\dagger\hat{\sigma}_{14}^j - g_2\hat{\sigma}_{23}^j\hat{a}, \tag{3j}
$$

$$
\dot{\hat{\sigma}}_{34}^j = -\tilde{\gamma}_{34}\hat{\sigma}_{34}^j + \Omega_c\hat{\sigma}_{24}^j - g_2\big(\hat{\sigma}_{33}^j - \hat{\sigma}_{44}^j\big)\hat{a}, \tag{3k}
$$

where $\tilde{\gamma}_{12} = i\Delta_{21} + \gamma_{12}$, $\tilde{\gamma}_{13} = i(\Delta_{21} - \Delta_{23}) + \gamma_{13}$, $\tilde{\gamma}_{34} = i\Delta_{43} + \gamma_{34}$, $\tilde{\gamma}_{24} = i(\Delta_{43} - \Delta_{23}) + \gamma_{24}$, $\tilde{\gamma}_{23} = -i\Delta_{23} + \gamma_{32}$, and $\tilde{\gamma}_{14} = i(\Delta_{21} - \Delta_{23} + \Delta_{43}) + \gamma_{14}$. We define $\gamma_{mn} = (\Gamma_n + \Gamma_m)/2$, with Γ_n (Γ_m) the total decay rate of population out of level $|n\rangle$ ($|m\rangle$).

The atomic degrees of freedom can be adiabatically eliminated [58], under the assumption that the spontaneous decay rates of the atoms are much larger than the atom-field coupling rates, i.e., $\Gamma_{nm} \gg g_1, g_2$, so that the atomic coherence and population operators $\hat{\sigma}_{mn}^j$ evolve much faster than $\hat{a}$ and reach their steady state much earlier than $\hat{a}$. Solving the steady-state solutions of $\hat{\sigma}_{12}^j$ and $\hat{\sigma}_{34}^j$ allow us to express the effective Hamiltonian and the additional decay process induced by atomic effects in terms of the mode operators. Under the condition that $g_1\langle\hat{a}\rangle$, $g_2\langle\hat{a}\rangle \ll \Omega_c$, the atomic operators can be

perturbatively expanded [59] as

$$\hat{\sigma}_{mn} = \hat{\sigma}_{mn}^{(0)} + \hat{\sigma}_{mn}^{(1)} + \hat{\sigma}_{mn}^{(2)} + \hat{\sigma}_{mn}^{(3)} + \cdots, \tag{4}$$

where we neglect the superscript j denoting the jth atom for convenience. Since the cavity mode couples weakly to each individual atom, each atom can be assumed to be populated at the ground state to zeroth order, i.e., $\hat{\sigma}_{11}^{(0)} = 1$, $\hat{\sigma}_{nn}^{(0)} = 0$ ($n = 2, 3, 4$), and $\hat{\sigma}_{mn}^{(0)} = 0$ ($m \neq n$). Under this assumption, we iteratively determine the remaining components of higher orders in the expansion [59]. Substituting the zeroth-order population and coherence into Eqs. (3h)–(3k) and (3b)–(3g), respectively, the first-order perturbation of the coherence and population operators can be obtained as

$$\hat{\sigma}_{12}^{(1)} = \frac{-g_1 \hat{a}}{\tilde{\gamma}_{12} + \frac{|\Omega_c|^2}{\tilde{\gamma}_{13}}}, \tag{5a}$$

$$\hat{\sigma}_{34}^{(1)} = \hat{\sigma}_{24}^{(1)} = 0, \tag{5b}$$

$$\hat{\sigma}_{nn}^{(1)} = \hat{\sigma}_{23}^{(1)} = \hat{\sigma}_{14}^{(1)} = 0 \quad (n = 1, 2, 3, 4). \tag{5c}$$

In a closed atomic system, the total population is conserved, i.e., $\hat{\sigma}_{11} + \hat{\sigma}_{22} + \hat{\sigma}_{33} + \hat{\sigma}_{44} = 1$. Then it can be deduced directly that

$$\hat{\sigma}_{11}^{(2)} + \hat{\sigma}_{22}^{(2)} + \hat{\sigma}_{33}^{(2)} + \hat{\sigma}_{44}^{(2)} = 0. \tag{6}$$

substituting Eqs. (5a) and (5b) into Eqs. (3b)–(3e) and combining with Eq. (6) and the assumption of $\hat{\sigma}_{23}^{(2)} = \hat{\sigma}_{14}^{(2)} = 0$, the second-order correction can be obtained as

$$\hat{\sigma}_{22}^{(2)} = \frac{g_1^2}{\Gamma_{21} + \Gamma_{23}} \frac{2\,\mathrm{Re}(F_1)}{|F_1|^2} a^{\dagger} a, \tag{7a}$$

$$\hat{\sigma}_{33}^{(2)} = g_1^2 \frac{\Gamma_{23}}{\Gamma_{31}(\Gamma_{21} + \Gamma_{23})} \frac{2\,\mathrm{Re}(F_1)}{|F_1|^2} a^{\dagger} a, \tag{7b}$$

$$\hat{\sigma}_{11}^{(2)} = -g_1^2 \frac{\Gamma_{23} + \Gamma_{31}}{\Gamma_{31}(\Gamma_{21} + \Gamma_{23})} \frac{2\,\mathrm{Re}(F_1)}{|F_1|^2} a^{\dagger} a, \tag{7c}$$

$$\hat{\sigma}_{44}^{(2)} = 0, \tag{7d}$$

$$\hat{\sigma}_{mn}^{(2)} = 0 \quad (m \neq n), \tag{7e}$$

where $F_1 = \tilde{\gamma}_{12} + |\Omega_c|^2/\tilde{\gamma}_{13}$. Similarly, substituting the second-order perturbation of the operators (7a)–(7e) into Eqs. (3h)–(3k), we obtain $\hat{\sigma}_{12}$ and $\hat{\sigma}_{34}$ to third order

$$\hat{\sigma}_{12}^{(3)} = g_1^3 \frac{\Gamma_{23} + 2\Gamma_{31}}{\Gamma_{31}(\Gamma_{21} + \Gamma_{23})} \frac{2\,\mathrm{Re}(F_1)}{F_1|F_1|^2} \hat{a}^{\dagger} \hat{a}^2, \tag{8a}$$

$$\hat{\sigma}_{34}^{(3)} = -g_2 g_1^2 \frac{\Gamma_{23}}{\Gamma_{31}(\Gamma_{21} + \Gamma_{23})} \frac{2\,\mathrm{Re}(F_1)}{F_2|F_1|^2} \hat{a}^{\dagger} \hat{a}^2, \tag{8b}$$

where $F_2 = \tilde{\gamma}_{34} + |\Omega_c|^2/\tilde{\gamma}_{24}$.

If $\hat{Q}(t)$ is an arbitrary combination of mode operators, the equation of motion for $\hat{Q}(t)$ is written from Eq. (1) combined with the Lindblad operator (2)

$$\dot{\hat{Q}} = i\Delta[\hat{Q}, \hat{a}^{\dagger} \hat{a}]$$

$$+ g_1[\hat{Q}, \hat{a}^{\dagger}] \sum_{j=1}^{N} \hat{\sigma}_{12}^{j} - g_1 \sum_{j=1}^{N} \hat{\sigma}_{21}^{j} [\hat{Q}, \hat{a}]$$

$$+ g_2[\hat{Q}, \hat{a}^{\dagger}] \sum_{j=1}^{N} \hat{\sigma}_{34}^{j} - g_2 \sum_{j=1}^{N} \hat{\sigma}_{43}^{j} [\hat{Q}, \hat{a}]$$

$$+ \frac{\kappa}{2} [2\hat{a}^{\dagger} \hat{Q} \hat{a} - \hat{a}^{\dagger} \hat{a} \hat{Q} - \hat{Q} \hat{a}^{\dagger} \hat{a}]$$

$$+ \sqrt{\kappa_{e1}} \varepsilon_p [\hat{Q}, \hat{a}^{\dagger} - \hat{a}]. \tag{9}$$

Substituting Eqs. (8a) and (8b) into Eq. (9) leads to

$$\dot{\hat{Q}} = i(\Delta - \delta\omega_{\mathrm{cav}})[\hat{Q}, \hat{a}^{\dagger} \hat{a}] - i\eta[\hat{Q}, \hat{a}^{\dagger 2} \hat{a}^2]$$

$$+ \frac{\kappa_a^{\mathrm{L}} + \kappa}{2} [2\hat{a}^{\dagger} \hat{Q} \hat{a} - \hat{a}^{\dagger} \hat{a} \hat{Q} - \hat{Q} \hat{a}^{\dagger} \hat{a}]$$

$$+ \frac{\kappa_a^{\mathrm{NL}}}{2} [2\hat{a}^{\dagger 2} \hat{Q} \hat{a}^2 - \hat{a}^{\dagger 2} \hat{a}^2 \hat{Q} - \hat{Q} \hat{a}^{\dagger 2} \hat{a}^2]$$

$$+ \sqrt{\kappa_{e1}} \varepsilon_p [\hat{Q}, \hat{a}^{\dagger} - \hat{a}], \tag{10}$$

where

$$\delta\omega_{\mathrm{cav}} = -g_1^2 N \frac{\mathrm{Im}(F_1)}{|F_1|^2}, \tag{11a}$$

$$\kappa_a^{\mathrm{L}} = 2g_1^2 N \frac{\mathrm{Re}(F_1)}{|F_1|^2}, \tag{11b}$$

$$\kappa_a^{\mathrm{NL}} = 4g_1^2 N \left[-g_1^2 Y_1 \frac{\mathrm{Re}(F_1)^2}{|F_1|^4} + g_2^2 Y_2 \frac{\mathrm{Re}(F_2)\mathrm{Re}(F_1)}{|F_2|^2 |F_1|^2} \right], \tag{11c}$$

$$\eta = 2g_1^2 N \left[g_1^2 Y_1 \frac{\mathrm{Im}(F_1)\mathrm{Re}(F_1)}{|F_1|^4} - g_2^2 Y_2 \frac{\mathrm{Im}(F_2)\mathrm{Re}(F_1)}{|F_2|^2 |F_1|^2} \right], \tag{11d}$$

with $Y_1 = (\Gamma_{23} + 2\Gamma_{31})/\Gamma_{31}(\Gamma_{21} + \Gamma_{23})$ and $Y_2 = \Gamma_{23}/\Gamma_{31}(\Gamma_{21} + \Gamma_{23})$ for N identical atoms.

We derive the effective Hamiltonian of the system from Eq. (10) to be

$$\hat{H} = (-\Delta + \delta\omega_{\mathrm{cav}})\hat{a}^{\dagger} \hat{a} + \eta\hat{a}^{\dagger 2} \hat{a}^2 + i\sqrt{\kappa_{e1}} \varepsilon_p(\hat{a}^{\dagger} - \hat{a}). \tag{12}$$

the one-photon decay process of the system, including the original decay process of the cavity mode and the additional one-photon absorption induced by atomic effects, is given by the effective linear Lindblad operator

$$\hat{\mathcal{L}}[\kappa^{\mathrm{L}}, \hat{a}]\hat{Q} = \frac{\kappa^{\mathrm{L}}}{2} [2\hat{a}^{\dagger} \hat{Q} \hat{a} - \hat{a}^{\dagger} \hat{a} \hat{Q} - \hat{Q} \hat{a}^{\dagger} \hat{a}], \tag{13}$$

where $\kappa^{\mathrm{L}} = \kappa + \kappa_a^{\mathrm{L}}$ is the overall linear decay rate of the cavity mode. The two-photon absorption process of the system is given by the effective nonlinear Lindblad operator

$$\hat{\mathcal{L}}[\kappa_a^{\mathrm{NL}}, \hat{a}]\hat{Q} = \frac{\kappa_a^{\mathrm{NL}}}{2} [2\hat{a}^{\dagger 2} \hat{Q} \hat{a}^2 - \hat{a}^{\dagger 2} \hat{a}^2 \hat{Q} - \hat{Q} \hat{a}^{\dagger 2} \hat{a}^2]. \tag{14}$$

Here κ_a^{NL} denotes the nonlinear dissipation resulting from the two-photon absorption. The PB effect in our dissipative scheme is critically dependent on the decay of Fock states $|n\rangle$, with $n = 0, 1, 2, \ldots$. Replacing the operator $\hat{Q}$ with $P_n|n\rangle\langle n|$, where P_n is the population of the state $|n\rangle$, the linear Lindblad operator in Eq. (13) contributes $n\kappa^{\mathrm{L}}$ to the decay rate of the state $|n\rangle$, while the nonlinear one contributes $(n-1)n\kappa_a^{\mathrm{NL}}$. This nonlinear term causes strong anharmonicity in the decay of the cavity mode, namely, the cavity impedance [60–62].

The first term in Eq. (12) indicates that the cavity atomic system is now simulated as a cavity with a dispersive refractive index, where the resonance frequency dispersively

changes versus the input field frequency. The resonance frequency of the cavity with a dispersive refractive index is $\omega_q = q2\pi c/n(\omega_q)L = q2\pi c/\sqrt{1 + (l_m/L)\mathrm{Re}(\chi^{(1)})(\omega_q)}L$, where L is the round-trip length of intracavity photons, l_m is the length traveled by a photon in the atomic medium in a round-trip, and $\chi^{(1)}$ is the linear atomic susceptibility. Then the resonance frequency of the equivalent dispersive cavity can be approximated as $\omega'_{\mathrm{cav}} \approx q2\pi c/L[1 - (l_m/2L)\mathrm{Re}(\chi^{(1)})(\omega'_{\mathrm{cav}})] \equiv \omega_{\mathrm{cav}} + \delta\omega_{\mathrm{cav}}(\omega'_{\mathrm{cav}})$ [63], in which $\omega_{\mathrm{cav}} \equiv q2\pi c/L$ is the bare cavity resonance and $\delta\omega_{\mathrm{cav}}(\omega'_{\mathrm{cav}})$ denotes the pulling of the bare cavity resonance which is induced by the atomic phase-shift effects.

For the case that the equivalent dispersive cavity is resonantly driven, i.e., $\omega_p = \omega'_{\mathrm{cav}}$, the detuning in the first term of Eq. (12) vanishes, as $-\Delta + \delta\omega_{\mathrm{cav}} = \omega_{\mathrm{cav}} - \omega'_{\mathrm{cav}} + \delta\omega_{\mathrm{cav}}(\omega'_{\mathrm{cav}}) = 0$. The related detunings are reduced to $\Delta_{21} = \omega_{21} - \omega'_{\mathrm{cav}}$ and $\Delta_{43} = \omega_{43} - \omega'_{\mathrm{cav}}$; then F_1 and F_2 in Eqs. (11a)–(11d) are reduced to functions of ω'_{cav} in the forms

$$F_1 = i(\omega_{21} - \omega'_{\mathrm{cav}}) + \gamma_{12} + \frac{|\Omega_c|^2}{i(\omega_{21} - \omega'_{\mathrm{cav}} - \Delta_{23}) + \gamma_{13}},$$

(15a)

$$F_2 = i(\omega_{43} - \omega'_{\mathrm{cav}}) + \gamma_{34} + \frac{|\Omega_c|^2}{i(\omega_{43} - \omega'_{\mathrm{cav}} - \Delta_{23}) + \gamma_{24}}.$$

(15b)

Therefore, the shift of the cavity resonance, the atomic one-photon absorption, and the two-photon nonlinearities are determined by the detunings Δ_{21} and Δ_{43} or, equivalently, the frequency ω'_{cav} of the actually resonant intracavity field.

For a slightly off-resonant frequency component in the probe laser, the detuning in the first term of Eq. (12) is written as $-\Delta + \delta\omega_{\mathrm{cav}} \equiv -\Delta' + \delta\omega_{\mathrm{cav}}(\omega_p) - \delta\omega_{\mathrm{cav}}(\omega'_{\mathrm{cav}})$, with the definitions $\Delta' \equiv \omega_p - \omega'_{\mathrm{cav}}$ and $\delta\omega_{\mathrm{cav}}(\omega'_{\mathrm{cav}}) \equiv \omega'_{\mathrm{cav}} - \omega_{\mathrm{cav}}$. We define $d(\delta\omega_{\mathrm{cav}})(\Delta') \equiv \delta\omega_{\mathrm{cav}}(\omega_p) - \delta\omega_{\mathrm{cav}}(\omega'_{\mathrm{cav}})$ as the effective cavity resonance including the atom-induced shift. Then the Hamiltonian (12) takes the form

$$\hat{H} = [-\Delta' + d(\delta\omega_{\mathrm{cav}})(\Delta')]\hat{a}^\dagger\hat{a} + \eta\hat{a}^{\dagger 2}\hat{a}^2 + i\sqrt{\kappa_{e1}}\varepsilon_p(\hat{a}^\dagger - \hat{a})$$

(16)

for the scanning probe field. In the response to the scanning probe field, $d(\delta\omega_{\mathrm{cav}})(\Delta')$, η, κ_a^{L}, and κ_a^{NL} change versus the detuning Δ' through $F_1(\Delta')$ and $F_2(\Delta')$, since the related detunings in F_1 and F_2 become $\Delta_{21} = \omega_{21} - \omega'_{\mathrm{cav}} - \Delta'$ and $\Delta_{43} = \omega_{43} - \omega'_{\mathrm{cav}} - \Delta'$, and thus F_1 and F_2 are determined only by the detuning Δ'.

III. MECHANISM OF NONLINEAR DISSIPATION-INDUCED PHOTON BLOCKADE

In this section we explain the mechanism of the PB induced by the two-photon absorption. The equal-time second-order correlation function at time t is $g^{(2)}(t) = \langle\hat{a}^{\dagger 2}\hat{a}^2\rangle(t)/\langle\hat{a}^\dagger\hat{a}\rangle^2(t)$, indicating the performance of the PB and the quantum statistical property of a single-photon field. Thus, it is of the most interest in our discussion.

We first discuss the influence of the linear dissipation on the correlation function $g^{(2)}$ without the external driving to the system. From the linear dissipation process described by
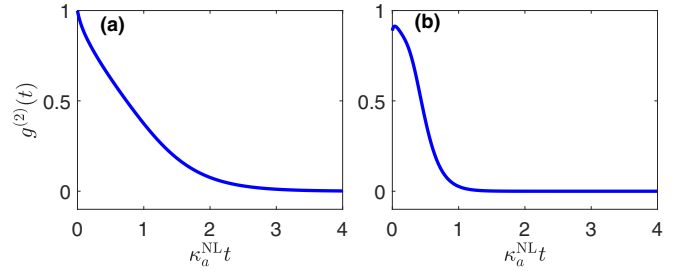
FIG. 2. Time evolution of the equal-time second-order correlation function during the two-photon absorption process from (a) the initial coherent state with mean photon number 4 and (b) the initial $|n = 9\rangle$ Fock state.

Eq. (13), we obtain

$$\frac{d\langle\hat{a}^{\dagger 2}\hat{a}^2\rangle}{dt} = -2\kappa^{\mathrm{L}}\langle\hat{a}^{\dagger 2}\hat{a}^2\rangle.$$

(17)

Here the expectation value of $\langle\hat{a}^{\dagger 2}\hat{a}^2\rangle$ implies the joint counting rate of two coincident photons. Clearly, it damps exponentially. Then the correlation function is constant,

$$g^{(2)}(t) = \frac{G_0}{\bar{n}_0^2},$$

(18)

where $G_0 = \langle\hat{a}^{\dagger 2}\hat{a}^2\rangle|_{t=0}$ and $\bar{n}_0 = \langle\hat{a}^\dagger\hat{a}\rangle|_{t=0}$. The two-photon correlation of an arbitrary initial cavity field remains unchanged in the linear dissipation process.

Now we discuss the correlation function when only the nonlinear dissipation is included. Instead of analyzing the time derivation $d\langle\hat{a}^{\dagger 2}\hat{a}^2\rangle/dt$, which involves higher-order operators, we calculate $d\langle\hat{a}^\dagger\hat{a}\rangle/dt$. The two-photon absorption process described by the Lindblad operator (14) gives

$$\frac{d\langle\hat{a}^\dagger\hat{a}\rangle}{dt} = -2\kappa_a^{\mathrm{NL}}\langle\hat{a}^{\dagger 2}\hat{a}^2\rangle.$$

(19)

In the steady state, we have $\langle\hat{a}^{\dagger 2}\hat{a}^2\rangle = 0$ and thus obtain $g_{\mathrm{ss}}^{(2)}(0) = 0$. This is caused by the two-photon absorption. In contrast to a linear dissipation process, an arbitrary initial state decays to a state only including the vacuum state and the single-photon state in the two-photon absorption process. In Fig. 2 we present the time evolution of an initial coherent state and an $|n = 9\rangle$ Fock state as an example. The time evolution of $g^{(2)}(t)$ confirms that two-photon absorption can cause a deep PB.

The underlying physics behind the dissipation-induced PB is schematically shown in Fig. 3. Under the driving of a coherent field ε_p, the cavity mode is excited from transitions of $|n\rangle \rightarrow |n + 1\rangle$. Taking a Fabry-Pérot cavity as an example for our explanation, we assume that the decay rates due to the two input and output channels are κ_e and the intrinsic loss rate of the cavity is κ_i. We consider the case of $\kappa_i \ll \kappa_e$ and $\kappa^{\mathrm{L}} = 2\kappa_e + \kappa_i$. In the linear dissipation case, the decay rate difference between the two successive Fock states is κ^{L}. The external resonant driving can be impedance matching [60,61]. On resonance, the Fock-state transition is driven at a strength of $2\kappa_e\varepsilon_p/(2\kappa_e + \kappa_i) \approx \varepsilon_p$. However, the impedance matching breaks when a large nonlinear dissipation (two-photon absorption here) is included. The two-photon absorption adds an
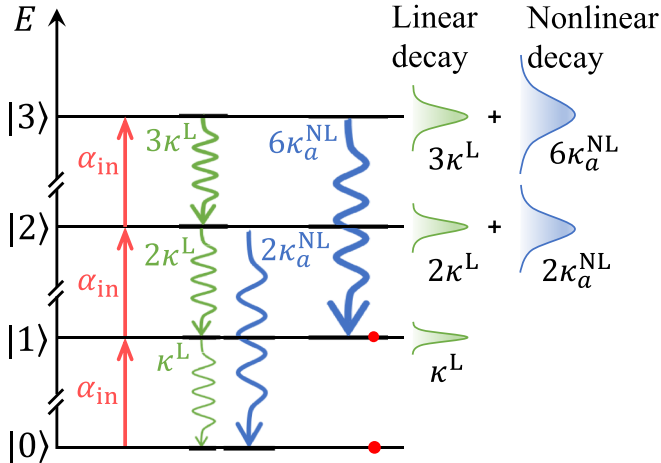
FIG. 3. Schematic for understanding the dissipation-induced PB. The cascaded red arrows show the single-photon pumping process of $|n\rangle \rightarrow |n+1\rangle$ transitions by the coherent field. The green (blue) arrows denote the one-photon (two-photon) decay. The green (blue) wave packets beside the Fock states represent the linewidths of the corresponding Fock state due to the linear and nonlinear dissipation.

extra nonlinear decay rate $(n-1)n\kappa_a^{\mathrm{NL}}$ to the Fock state $|n \geqslant 2\rangle$ of the cavity mode. This extra decay causes impedance mismatching to the transitions of $|n\rangle \rightarrow |n+1\rangle$ for $n \geqslant 1$. For $\kappa_a^{\mathrm{NL}} \gg \kappa^{\mathrm{L}}$, the excitation probability of $|n\rangle \rightarrow |n+1\rangle$ with $n > 1$ reduces to $|2\kappa_e/(2\kappa_e + \kappa_i + 2\kappa_a^{\mathrm{NL}}\hat{a}^\dagger\hat{a})|^2$. In the nonlinear dispersive scheme, this excitation probability is given by $|2\kappa_e/(2i\eta\hat{a}^\dagger\hat{a} + 2\kappa_e + \kappa_i)|^2$. As a result, two-photon absorption prevents the excitation of Fock states $|n \geqslant 2\rangle$ by the coherent driving field. Only one photon can enter and pass the cavity each time. This is the mechanism leading to the PB effect here.

We also study the distribution of photon-number states during the PB by solving the cascaded quantum master equation (see Appendix B for details), as shown in Fig. 4. In this model, we consider a source cavity mode $\hat{d}$ and an acceptor cavity mode $\hat{a}$, connected by a one-way quantum bus leading a quantum field $\hat{b}$. Here the input coherent field ε_p in the normal master equation needs to be replaced by a quantum field with $\hat{b} = \sqrt{\kappa_{d2}}\hat{d}$, where $\hat{d}$ is the annihilation operator of the source cavity mode. Here the mean photon number of the source cavity is 2 within a period of κ_{d1}^{-1}. The input photon-number distribution of the acceptor cavity is shown in Fig. 4(a). The photon-number distribution of the cavity mode is shown in Fig. 4(b). It can be seen that the cavity has only the quantum vacuum state and the single-photon state ($P_1 = 0.4$). The transmitted mode is the same as the cavity mode. Thus, only the single-photon state exists in the transmission. The reflected mode is presented in Fig. 4(c). The mean photon number of the reflected mode is about 0.65. The multiphoton components in the reflected mode are reduced in comparison with the Poissonian input field.

IV. RESULTS

As proposed by Imamoğlu and co-workers [22,23], a large Kerr nonlinearity based on electromagnetically induced
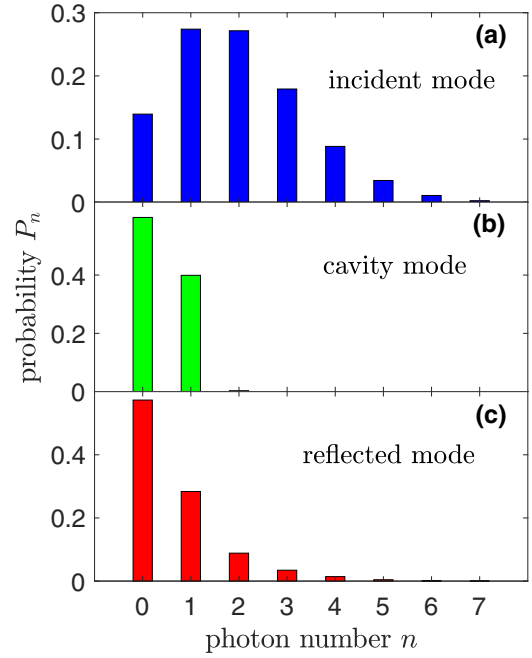
FIG. 4. Steady-state photon-number distribution of (a) the source mode, (b) the acceptor cavity mode, and (c) the reflected mode for a resonantly driven acceptor cavity with nonlinear dissipation. The other parameters are $\kappa_{d1} = \kappa_{d2} = \kappa_{e1} = \kappa_{e2} = \kappa/2$ (with κ the bare-cavity decay rate), $\kappa_a^{\mathrm{L}} = 0$, $\kappa_a^{\mathrm{NL}} = 10\kappa$, and $|\alpha(t)|^2/\kappa_{d1} = 2$.

transparency (EIT) has several advantages, including atomic one-photon loss elimination and vanishing shift of the resonance frequency. If the cavity field at the resonance frequency ω_{cav} and the coupling laser at ω_c are at two-photon resonance with the $|1\rangle \leftrightarrow |3\rangle$ transition, the transparency or a dark resonance is created at the cavity-mode frequency. In Fig. 5 the dispersion-induced shift of the bare cavity resonance $\delta\omega_{\mathrm{cav}}(\omega'_{\mathrm{cav}})$ and the one-photon atomic absorption rate κ_a^{L} are plotted versus the effective resonance frequency ω'_{cav}, under the condition that the coupling field is resonant with the $|3\rangle \leftrightarrow |2\rangle$ transition. It is verified from Fig. 5(b) that the atomic one-photon absorption rate is negligibly small (about $0.028\,12\kappa$) when the intracavity field with frequency ω'_{cav} is also resonant with the $|1\rangle \leftrightarrow |2\rangle$ transition. Meanwhile, the pulling of the bare cavity resonance vanishes, as shown in Fig. 5(a), which indicates a canceled linear atomic polarization of the $|1\rangle \leftrightarrow |2\rangle$ transition. Since the EIT scheme has these advantages, we use the two-photon resonance condition in the following context to eliminate linear atomic polarization and preserve third-order nonlinear polarization simultaneously, so as to avoid pulling the bare cavity resonance frequency and obtain a negligible one-photon absorption.

In Fig. 6 the Kerr nonlinear coefficient η and the two-photon absorption rate κ_a^{NL} are plotted as functions of the detuning between the $|3\rangle \leftrightarrow |4\rangle$ transition and the pulled resonance frequency ω'_{cav} under the two-photon resonance condition. We set the detuning between the $|1\rangle \leftrightarrow |2\rangle$ and $|3\rangle \leftrightarrow |4\rangle$ transitions to be 4560κ and the two-photon resonance condition is taken as $\omega_{21} - \omega'_{\mathrm{cav}} = \Delta_{23} = 4560\kappa$ to make the cavity field nearly resonantly coupled to the $|3\rangle \leftrightarrow |4\rangle$ transition. To realize antibunched photons via the two-
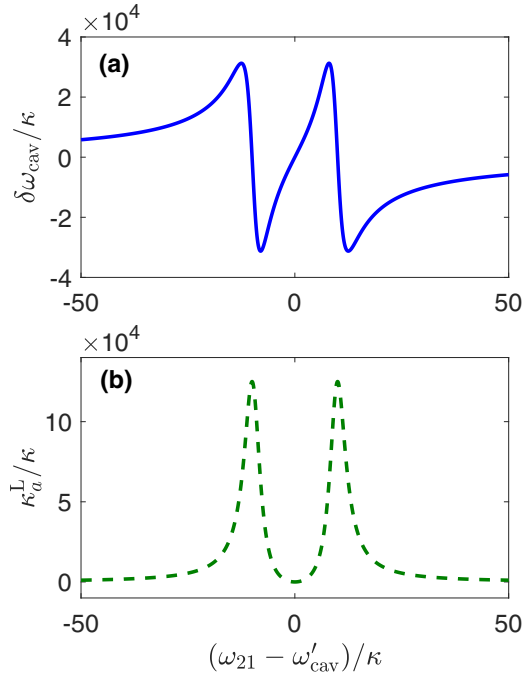
FIG. 5. (a) Resonance frequency shift $\delta\omega_{\text{cav}}$ and (b) one-photon absorption rate κ_a^{L} as a function of the pulled cavity resonance frequency ω'_{cav}, under the condition that the coupling laser is resonant with the $|3\rangle \leftrightarrow |2\rangle$ transition. We use $N = 12.5 \times 10^6$, $g_1/\kappa = 0.15$, $\Omega_c/\kappa = 10$, $\Gamma_{31}/\kappa = 10^{-5}$, $\Gamma_{21}/\kappa = \Gamma_{23}/\kappa = 4.5$, $\omega_p = \omega'_{\text{cav}}$, and $\Delta_{23} = 0$.

photon absorption instead of a conservative Kerr nonlinearity, we want a nearly imaginary $\chi^{(3)}$ nonlinearity. Therefore, we choose the parametric point corresponding to $\eta/\kappa \approx 0$, marked by a blue circle with the detuning $\omega_{43} - \omega'_{\text{cav}} = -0.0219\kappa$ and $\eta/\kappa \sim 10^{-4}$, as shown in Fig. 6. The relevant nonlinear dissipation rate is $\kappa_a^{\text{NL}}/\kappa = 28.12$, which is marked by a green circle. The related one-photon absorption rate and the pulling of the resonance frequency are $\kappa_a^{\text{L}}/\kappa = 0.028\,12$ and $\delta\omega_{\text{cav}}(\omega'_{\text{cav}})/\kappa \sim 10^{-6}$, respectively. We take the parameter configuration of $\omega_{21} - \omega'_{\text{cav}} = \Delta_{23} = 4560\kappa$ and $\omega_{43} -$
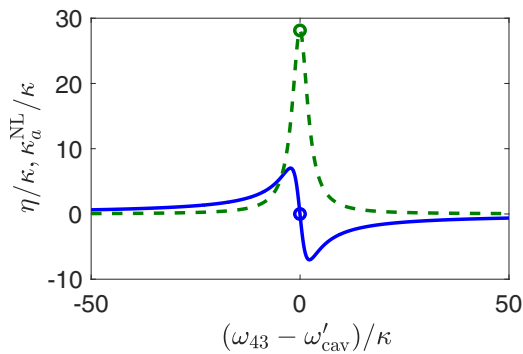
FIG. 6. Kerr nonlinear coefficient η (solid line) and two-photon absorption rate κ_a^{NL} (dashed line) versus the detuning between the $|3\rangle \leftrightarrow |4\rangle$ transition and the pulled resonance frequency ω'_{cav} under the two-photon resonance condition. The parameters are $N = 12.5 \times 10^6$, $g_1/\kappa = g_2/\kappa = 0.15$, $\Omega_c/\kappa = 10$, $\Gamma_{31}/\kappa = 10^{-5}$, $\Gamma_{21}/\kappa = \Gamma_{23}/\kappa = \Gamma_{43}/\kappa = 4.5$, and $(\omega_{21} - \omega'_{\text{cav}})/\kappa = \Delta_{23}/\kappa = 4560$.
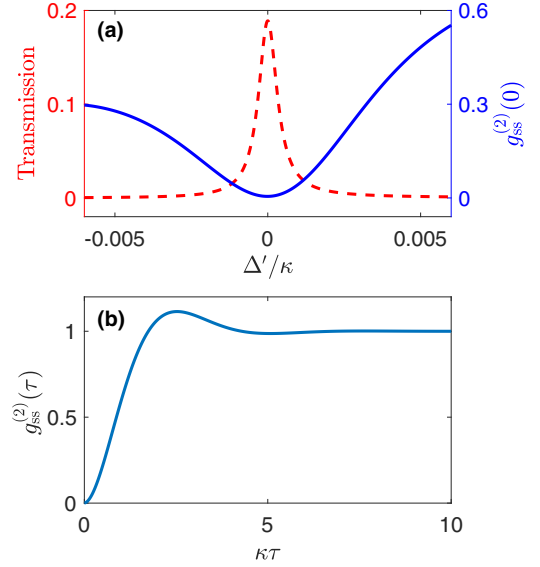
FIG. 7. (a) Transmission of the cavity field (dashed line) and the equal-time second-order correlation function at the steady state $g_{\text{ss}}^{(2)}(0)$ (solid line) versus the detuning Δ' between the probe laser and the modified resonance and (b) the steady-state second-order correlation function with delay time τ versus the delay time. The parameters are $N = 12.5 \times 10^6$, $g_1/\kappa = g_2/\kappa = 0.15$, $\Omega_c/\kappa = 10$, $\Gamma_{31}/\kappa = 10^{-5}$, $\Gamma_{21}/\kappa = \Gamma_{23}/\kappa = \Gamma_{43}/\kappa = 4.5$, $(\omega_{21} - \omega'_{\text{cav}})/\kappa = \Delta_{23}/\kappa = 4560$, and $(\omega_{43} - \omega'_{\text{cav}})/\kappa = -0.0219$, which lead to $\kappa_a^{\text{L}}/\kappa = 0.02812$, $\eta/\kappa \sim 10^{-4}$, and $\kappa_a^{\text{NL}}/\kappa = 28.12$ for the resonant probe field. In addition, $\kappa_{e1}/\kappa = \kappa_{e2}/\kappa = 0.45$, $\kappa_i/\kappa = 0.1$, and $\varepsilon_p = \sqrt{2\kappa_{e1}}$.

$\omega'_{\text{cav}} = -0.0219\kappa$ in the following context, which leads to a resonantly driven cavity with a negligible linear atomic effect and a large, purely absorptive two-photon nonlinearity. To briefly summarize, one-photon state propagates without loss as in vacuum, as the atomic medium is reduced to its Λ-type subsystem for one-photon excitation, where EIT eliminates one-photon absorption, whereas for the simultaneous arrival of two or more photons, the complete N-type level structure works, by which the two-photon absorption is switched on.

Then we explore the properties of the transmission spectrum and the steady-state second-order correlation function when the probe light scans around the modified resonance frequency. The transmission of photons is defined as $T = \langle \hat{a}_{\text{out}}^\dagger \hat{a}_{\text{out}} \rangle / |\varepsilon_p|^2$, where $\hat{a}_{\text{out}} = \sqrt{\kappa_{e2}}\hat{a}$ is the annihilation operator of the transmitted field. It is shown in Fig. 7(a) that the cavity linewidth of the transmission is significantly narrowed, which can be illustrated by the dispersive refractive index. As known from Eq. (16), although the detuning between the probe laser and the effective cavity resonance is Δ', the actual detuning is modified by the dispersive shift of the effective cavity resonance versus the scanning probe frequency, which is defined as $d(\delta\omega_{\text{cav}}) \equiv \delta\omega_{\text{cav}}(\omega_p) - \delta\omega_{\text{cav}}(\omega'_{\text{cav}})$ in Eq. (16). As shown in Fig. 11(a) of Appendix A, the dispersive shift of the effective cavity resonance is very sharp versus scanning probe frequency, which switches a slightly off-resonant frequency component out of the cavity resonance, leading to the significant cavity linewidth narrowing (see Appendix A for a detailed derivation). For the probe field scanning through the

narrowed cavity linewidth, the Kerr nonlinear coefficient and the atomic one-photon absorption rate are always negligible compared with the cavity decay rate, while the two-photon absorption rate remains large, as shown in Figs. 11(b)–(d) of Appendix A. Namely, the N-type quantum system can be modeled as a cavity with a dispersive refractive index which has a large two-photon absorption process in the response to the scanning probe field. The equal-time second-order correlation function at the steady state, which is defined as $g_{ss}^{(2)}(0) = \lim_{t\to\infty}\langle\hat{a}^\dagger\hat{a}^\dagger\hat{a}\hat{a}\rangle(t)/\langle\hat{a}^\dagger\hat{a}\rangle^2(t)$, measures the variance of the photon-number distribution of the cavity field and represents the probability of two-photon transmission. It is shown in Fig. 7(a) that $g_{ss}^{(2)}(0)$ reaches its minimum about 0.005 at the resonance and $g_{ss}^{(2)}(0) < 0.05$ within the narrowed cavity linewidth, indicating that the transmitted photons are well antibunched and sub-Poissonian when the probe laser drives the nonlinearly dissipative cavity within the linewidth. The steady-state second-order correlation function with time delay τ, which gives the joint probability of detecting a second photon at time τ given a detection event that starts from the steady state at time $t = 0$, is defined as $g_{ss}^{(2)}(\tau) = \lim_{t\to\infty}\langle\hat{a}^\dagger(t)\hat{a}^\dagger(t+\tau)\hat{a}(t+\tau)\hat{a}(t)\rangle/\langle\hat{a}^\dagger\hat{a}\rangle^2(t)$. In Fig. 7(b) $g_{ss}^{(2)}(\tau)$ is plotted versus the delay time τ for the resonantly driven system. It is shown that $g_{ss}^{(2)}(\tau)$ increases with the delay time, indicating photons are more likely to arrive separated in time, which verifies that the sub-Poissonian photons transmitted within the cavity linewidth are indeed antibunched.

The N-type atoms are widely used to achieve giant photon nonlinearity. To confirm the advantage of the nonlinear-dissipation (dissipative) scheme in PB over the nonlinear-dispersion (dispersive) scheme, we calculate the Kerr nonlinearity, the corresponding transmission, and the correlation function using the same atomic and cavity parameter regime as for dissipative nonlinearity. To do so, we take a different detuning of the $|3\rangle \leftrightarrow |4\rangle$ atomic transition in the parameter regime of the system, to obtain the maximal nonlinear dispersion for a resonant probe field. The transmission and the second-order correlation function are shown in Fig. 8 for comparison with the dissipative scheme. In comparison, we consider two cases: (i) the pure dispersive case and (ii) the combination case with both off-resonance dispersive and dissipative nonlinearities. In the first case, the two-photon absorption rate is set to zero to ensure that the PB is completely induced by the dispersive Kerr nonlinearity [see Fig. 8 (solid lines)]. In the second case, we keep both the calculated Kerr nonlinearity $\eta/\kappa = 7$ and the dissipative nonlinearity $\kappa_a^{NL}/\kappa = 13.9$. In comparison with the dissipative case shown in Fig. 7(a), the dispersive case has a very close transmission spectrum. However, the equal-time second-order correlation function, as an indicator of the PB effect, in latter case is considerably larger than that in the former. The function $g_{ss}^{(2)}(0)$ in the dispersive scheme reaches the minimal value of about 0.02 at $\Delta'/\kappa \sim 0$ [see the solid curve in Fig. 8(b)]. Although this value is already small, it is still about one order larger than the minimum 0.005 in the dissipative scheme [see Fig. 7(a)]. In this sense, the nonlinear-dissipation scheme using the same atom-cavity system is more efficient in PB than the nonlinear dispersion.

Below we discuss how the PB effect depends on the system parameters such as the mean photon flux $|\varepsilon_p|^2$ of the input
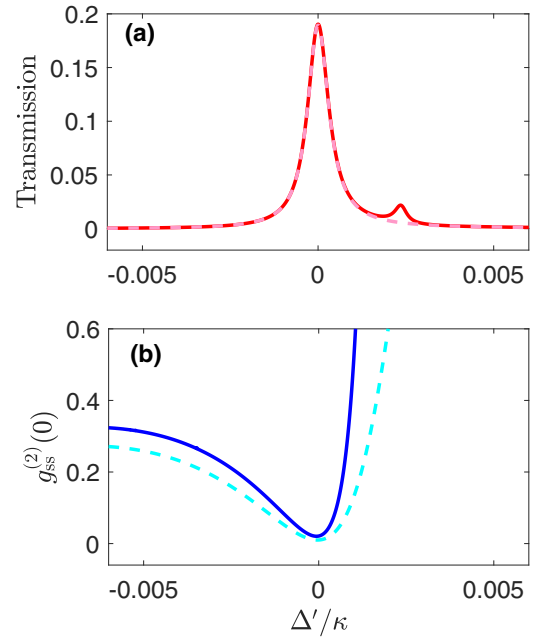
FIG. 8. (a) Overall transmission and (b) correlation function $g_{ss}^{(2)}(0)$ for the maximally available dispersive nonlinearity $\eta/\kappa = 7$ in an atomic ensemble of $N = 12.5 \times 10^6$. Solid curves are for the case without the two-photon absorption, $\kappa_a^{NL} = 0$ when scanning the detuning Δ', while dashed curves are for $\kappa_a^{NL}/\kappa = 13.9$ with a resonant probe field. Here $(\omega_{43} - \omega'_{cav})/\kappa = -2.3$, which leads to $\eta/\kappa = 7$ for a resonant probe field, and $|\varepsilon_p|^2/\kappa_{e1} = 2$.

coherent field and the number N of the atoms. The two-photon absorption rate κ_a^{NL} is proportional to N [see Eq. (11)]. Meanwhile, the one-photon absorption and linear and nonlinear dispersion of the atomic ensemble are negligible compared to the bare-cavity decay rate κ.

The populations P_1 and P_2 of single- and two-photon states are plotted in Fig. 9(a). We only show P_1 and P_2 because Fock states $|n \geqslant 3\rangle$ are negligibly excited. The population P_2 decrease quickly from 2.75% to 0.15% with N increasing to 6×10^6. In contrast, the population P_1 decreases slightly from 39.4% to 38%. After this point, P_1 goes down slowly and linearly as N increases. Consequently, the weight of single-photon excitation in all photon excitations $P_1/(1 - P_0)$ quickly becomes saturated, almost reaching unity [see the red dashed curve in Fig. 9(b)]. Here P_0 is the population of the vacuum state of the cavity mode. Correspondingly, the function $g_{ss}^{(2)}(0)$ approaches zero with N increasing [see the blue solid curve in Fig. 9(b)]. At $N = 6 \times 10^6$, we obtain $g_{ss}^{(2)}(0) \approx 0.02$ and $P_1 = 38\%$ in the dissipative scheme. In comparison, the dispersive scheme yields $g_{ss}^{(2)}(0) = 0.084$ and $P_1 = 38.3\%$.

The populations of different Fock states as a function of the mean photon flux $|\varepsilon_p|^2$ of the incident field are shown in Fig. 10(a). The population P_1 of the single-photon state quickly reaches a saturated value of 47% with the intensity of the input field. However, the population P_2 linearly increases. As a result, the weight of the single-photon state decreases linearly from almost unity, as shown in Fig. 10(b). The correlation function $g_{ss}^{(2)}(0)$ also increases linearly from nearly zero to 0.02 at $|\varepsilon_p|^2/\kappa_{e1} = 10$, implying the PB effect be-
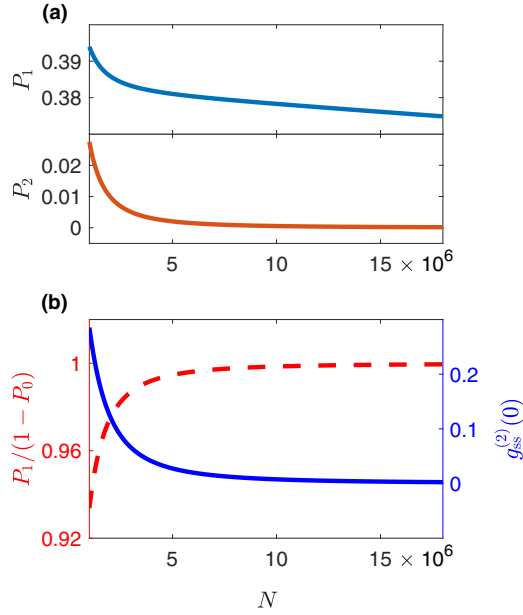
FIG. 9. (a) Populations P_1 (upper panel) and P_2 (lower panel) of single- and two-photon states versus the atom number N. (b) Weight $P_1/(1 - P_0)$ (dashed line) of single-photon excitation in all $|n \geqslant 1\rangle$ states and $g_{\text{ss}}^{(2)}(0)$ (solid line) versus the atom number N. The other parameters are $g_1/\kappa = g_2/\kappa = 0.15$, $\Omega_c/\kappa = 10$, $\Gamma_{31}/\kappa = 10^{-5}$, $\Gamma_{21}/\kappa = \Gamma_{23}/\kappa = \Gamma_{43}/\kappa = 4.5$, $(\omega_{21} - \omega'_{\text{cav}})/\kappa = \Delta_{23}/\kappa = 4560$, $(\omega_{43} - \omega'_{\text{cav}})/\kappa = -0.022$, $\kappa_{e1}/\kappa = \kappa_{e2}/\kappa = 0.45$, $\kappa_i/\kappa = 0.1$, and $|\varepsilon_p|^2/\kappa_{e1} = 2$.

comes weaker. Thus, the population of the single-photon state increases but its purity decreases as the input field becomes stronger. Nevertheless, we can obtain strong PB yielding $g_{\text{ss}}^{(2)}(0) < 0.02$ even when $|\varepsilon_p|^2/\kappa_{e1} < 10$.

V. EXPERIMENTAL IMPLEMENTATION

Our scheme can be implemented with a setup of a FP cavity with a ^{87}Rb cell placed inside, as depicted in Fig. 1(a). The two mirrors have the same reflectivity of 99%. End faces of the atomic cell are coated with 99.9% antireflection layers for the cavity mode. We use the 0.4-m-long FP cavity. The cavity internal losses is calculated to be $\kappa_i = 2\pi \times 0.12$ MHz and the external loss rates at the two ports are $\kappa_{e1} = \kappa_{e2} = 2\pi \times 0.6$ MHz, yielding $\kappa = 2\pi \times 1.32$ MHz. We exploit the D_1 line of the ^{87}Rb atom to realize the N-type configuration with $|1\rangle = |5\,^2S_{1/2}, F = 1, m_F = -1\rangle$, $|3\rangle = |5\,^2S_{1/2}, F = 2, m_F = -2\rangle$, $|2\rangle = |5\,^2P_{1/2}, F' = 1, m'_F = -1\rangle$, and $|4\rangle = |5\,^2P_{1/2}, F' = 2, m'_F = -2\rangle$. The coupling laser is left circularly polarized and the probe laser is linearly polarized. The single-photon atomic coupling strength is calculated to be about $g_1 = g_2 = 2\pi \times 0.2$ MHz for the mode volume of this cavity and the dipole matrix element of D_1 transition. In the related hyperfine levels in the D_1 line of ^{87}Rb atoms, the detuning between the $|1\rangle \leftrightarrow |2\rangle$ and $|3\rangle \leftrightarrow |4\rangle$ transitions is about $2\pi \times 6020$ MHz; thus we set the detuning between the $|1\rangle \leftrightarrow |2\rangle$ and $|3\rangle \leftrightarrow |4\rangle$ transitions to be 4560κ in the previous context. The decay rates of the hyperfine-level transitions in the ^{87}Rb D_1 line are about $2\pi \times 6$ MHz.
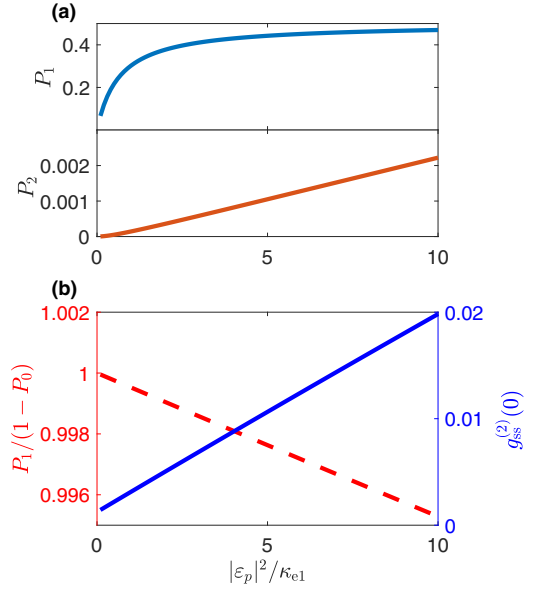
FIG. 10. (a) Populations P_1 (upper panel) and P_2 (lower panel) versus the mean input photon flux $|\varepsilon_p|^2$. (b) Weight of single-photon excitation $P_1/(1 - P_0)$ (dashed line) and $g_{\text{ss}}^{(2)}(0)$ (solid line) versus the mean input photon flux. The other parameters are the same as in Fig. 9 except for $N = 12.5 \times 10^6$.

VI. DISCUSSION AND CONCLUSION

N-type systems are usually exploited to realize a giant Kerr nonlinearity owing to the canceled linear susceptibility and the enhanced nonlinear susceptibility in the EIT scheme. Subsequently, the PB effect induced by absorptive-free nonlinear dispersion has been extensively researched; the mechanism behind it is that the large nonlinear phase shifts of multiphotons enable an anharmonic eigenenergy level structure of photons. However, the dispersive Kerr nonlinearity is suppressed by the large detuning in the nonresonant case. Counterintuitively, we eliminate the Kerr nonlinearity but keep a significant two-photon absorption by selecting near-resonant optical nonlinear processes. In such a configuration, we achieve deep PB. Our scheme for nonlinear dissipation-induced PB is easier to implement and more efficient.

In summary, we have proposed a scheme to realize the deep PB effect by inducing the large nonlinear dissipation of an optical cavity with N-type atoms. In particular, a large and dominant two-photon absorption is achieved in the cavity by means of a near-resonant nonlinear process, whereas the atomic one-photon absorption is suppressed to be vanishing. The deep PB is accessible within the linewidth of the N-type quantum system, which is completely induced by the nonlinear dissipation, and a high transmission efficiency is shown simultaneously. The nonlinear-dissipation scheme in our proposal is demonstrated to be more efficient in inducing the strong PB than the dispersive scheme using the same atom-cavity system. The effect of the nonlinear dissipation-induced PB becomes stronger with the atom number N, but it gets weaker with the mean photon flux $|\varepsilon_p|^2$. Our proposal provides a potential protocol for the efficient PB and may provide an alternate route towards manipulation of single photons.
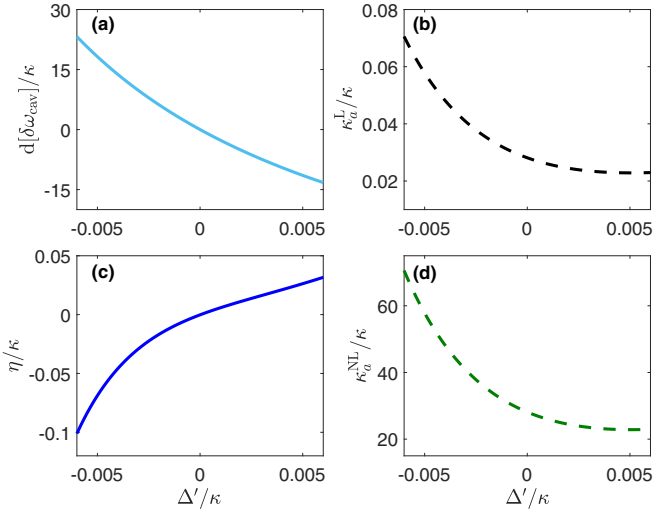
FIG. 11. (a) Dispersive shift of the effective cavity resonance, (b) atomic one-photon absorption rate, (c) Kerr nonlinear coefficient, and (d) atomic two-photon absorption rate versus the detuning Δ'. All the parameters are the same as in Fig. 7.

ACKNOWLEDGMENTS

APPENDIX A: CAVITY-LINEWIDTH NARROWING

The dispersive shift of the effective optical resonance, the Kerr nonlinear coefficient, and the atomic one-photon and two-photon absorption rates vary versus the detuning Δ' as shown in Fig. 11. A slightly off-resonant probe frequency with detuning $\Delta' = -0.005\kappa$ can see a large dispersive shift of the effective cavity resonance up to $d(\delta\omega_{\text{cav}}) = 18.22\kappa$, which switches itself out of the cavity resonance, leading to the significant cavity linewidth narrowing effect. The Kerr nonlinear coefficient and the atomic one-photon absorption rate are always negligibly small compared to the cavity decay rate when the probe frequency scans through the narrowed linewidth, as shown in Figs. 11(b) and 11(c). Nevertheless, the two-photon absorption rate is always large within the linewidth, as shown in Fig. 11(d).

We briefly deduce the cavity linewidth narrowing effect to better understand the results in the main text. Suppose the atomic medium with the linear susceptibility $\chi(\omega) = \chi'(\omega) + i\chi''(\omega)$ and the length $l_m/2$ is placed in the FP cavity of length $L/2$. Inside the atomic medium, the propagation constant of the radiation field is $\beta_m = \beta_0\sqrt{1 + \chi'(\omega)} \approx \beta_0 + \Delta\beta_m(\omega)$, where $\Delta\beta_m(\omega) = \beta_0\chi'(\omega)/2$ and β_0 is the propagation constant in the air. The round-trip phase shift $\phi(\omega)$ in the cavity is

$$\phi(\omega) = \frac{\omega}{c}L + \frac{\omega\chi'(\omega)}{2c}l_m. \tag{A1}$$

The complex amplitude of the circulating intracavity field is related to that of the incident field outside the cavity by

$$\tilde{E}_{\text{circ}} = it_1\tilde{E}_{\text{inc}} + \tilde{g}_{\text{rt}}(\omega)\tilde{E}_{\text{circ}}, \tag{A2}$$

where $\tilde{g}_{\text{rt}}(\omega) = r_1 r_2 e^{-\alpha L - i(\omega L/c + \omega\chi'(\omega)l_m/2c)}$, with r_1, t_1, r_2, and α the reflection and transmission coefficients of the input-port mirror, the reflection coefficient of the second mirror, and the attenuation constant inside cavity, respectively. The ratio of the complex amplitude of the circulating intracavity field to that of the incident field is given by

$$\frac{\tilde{E}_{\text{circ}}}{\tilde{E}_{\text{inc}}} = \frac{it_1}{1 - \tilde{g}_{\text{rt}}(\omega)}. \tag{A3}$$

The spectrum of the intracavity field is

$$
\begin{aligned}
T &= \frac{|t_1|^2}{|1 - \tilde{g}_{\text{rt}}(\omega)|^2} \\
&= \frac{|t_1|^2}{(1 - g_{\text{rt}})^2 + 4g_{\text{rt}}\sin^2[\omega L/2c + \omega\chi'(\omega)l_m/4c]},
\end{aligned} \tag{A4}
$$

where $g_{\text{rt}} = |\tilde{g}_{\text{rt}}|$. The intracavity field intensity reduces to half its maximum value when the frequency satisfies

$$\frac{\omega L}{2c} + \frac{\omega\chi'(\omega)}{4c}l_m = q\pi \pm \arcsin\left(\frac{1 - g_{\text{rt}}}{2\sqrt{g_{\text{rt}}}}\right); \tag{A5}$$

thus the frequencies corresponding to the half intracavity field intensity are

$$
\begin{aligned}
\omega_\pm &= \frac{q2\pi c/L \pm 2c/L\arcsin\left(\frac{1-g_{\text{rt}}}{2\sqrt{g_{\text{rt}}}}\right)}{1 + \frac{\chi'(\omega_\pm)l_m}{2L}} \\
&= \left[q\frac{2\pi c}{L} \pm \frac{2c}{L}\arcsin\left(\frac{1-g_{\text{rt}}}{2\sqrt{g_{\text{rt}}}}\right)\right] \\
&\quad \times \left[1 - \frac{l_m}{L}\frac{\chi'(\omega_\pm)}{2}\right],
\end{aligned} \tag{A6}
$$

leading to

$$\omega_+ = \left(\omega_{\text{cav}} + \frac{\Delta\omega}{2}\right)\left(1 - \frac{l_m}{2L}\chi'(\omega_+)\right), \tag{A7a}$$

$$\omega_- = \left(\omega_{\text{cav}} - \frac{\Delta\omega}{2}\right)\left(1 - \frac{l_m}{2L}\chi'(\omega_-)\right), \tag{A7b}$$

where $\omega_{\text{cav}} = q2\pi c/L$ is the bare cavity resonance frequency and $\Delta\omega = 4c/L\arcsin[(1 - g_{\text{rt}})/2\sqrt{g_{\text{rt}}}]$ is the linewidth of the bare cavity. Thus the modified cavity linewidth is obtained as

$$
\begin{aligned}
\Delta\omega' &= \omega_+ - \omega_- \\
&\approx -\frac{l_m}{2L}\omega_{\text{cav}}\chi'(\omega_+) + \frac{l_m}{2L}\omega_{\text{cav}}\chi'(\omega_-) + \Delta\omega \\
&< \Delta\omega.
\end{aligned} \tag{A8}
$$

In this equation we use the condition that $\chi'(\omega_+) > 0$ and $\chi'(\omega_-) < 0$. The modified cavity linewidth is narrowed compared to the bare cavity linewidth.
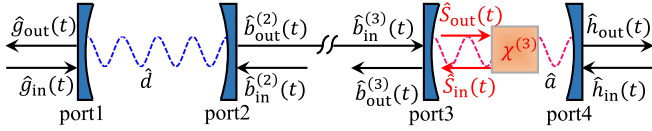
FIG. 12. Schematic diagram of the cascaded quantum system. The output of the first cavity at port 2 is guided to drive the second cavity at port 3. The second cavity contains atomic ensembles and thus experiences a nonlinear dissipation process.

APPENDIX B: CASCADED QUANTUM MODEL TO CHARACTERIZE THE INPUT OF THE NONLINEARLY DISSIPATIVE CAVITY

To investigate the statistics of the reflected field of the nonlinearly dissipative cavity, the incident field should be quantized radiation. We consider a cascaded quantum system [64–66] which can be decomposed into two subsystems, as depicted in Fig. 12. The first subsystem is an empty source cavity driven by the coherent light from port 1, whose fluorescent output from port 2 is fed into the input port of the second subsystem, namely, the localized nonlinearly dissipative acceptor cavity. The Hamiltonian for the cascaded system is

$$
\begin{aligned}
\hat{H} = & \hat{H}_{\text{sys}} + \int_{-\infty}^{\infty} d\omega\, \omega \hat{g}^\dagger(\omega)\hat{g}(\omega) + \int_{-\infty}^{\infty} d\omega\, \omega \hat{b}^\dagger(\omega)\hat{b}(\omega) \\
& + \int_{-\infty}^{\infty} d\omega\, \omega \hat{h}^\dagger(\omega)\hat{h}(\omega) + \int_{-\infty}^{\infty} d\omega\, \omega \hat{S}^\dagger(\omega)\hat{S}(\omega) \\
& + i \int_{-\infty}^{\infty} d\omega\, \gamma_1(\omega)\{\hat{g}^\dagger(\omega)\hat{d} - \hat{d}^\dagger \hat{g}(\omega)\} \\
& + i \int_{-\infty}^{\infty} d\omega\, \gamma_2(\omega)\{\hat{b}^\dagger(\omega)\hat{d} - \hat{d}^\dagger \hat{b}(\omega)\} \\
& + i \int_{-\infty}^{\infty} d\omega\, \gamma_3(\omega)\{\hat{b}^\dagger(\omega)e^{-i\omega\tau}\hat{a} - \hat{a}^\dagger \hat{b}(\omega)e^{i\omega\tau}\} \\
& + i \int_{-\infty}^{\infty} d\omega\, \gamma_4(\omega)\{\hat{h}^\dagger(\omega)\hat{a} - \hat{a}^\dagger \hat{h}(\omega)\} \\
& + i \int_{-\infty}^{\infty} d\omega\, G(\omega)\{\hat{S}^\dagger(\omega)\hat{a}^2 - \hat{a}^{\dagger 2}\hat{S}(\omega)\},
\end{aligned}
\tag{B1}
$$

where the quantum field $\hat{b}$ in the quantum data bus includes the modes $\hat{b}_{\text{in}}^{(2)}$, $\hat{b}_{\text{out}}^{(2)}$, $\hat{b}_{\text{in}}^{(3)}$, and $\hat{b}_{\text{out}}^{(3)}$; $\gamma_j(\omega)$ with $j = 1, 2, 3, 4$ represents the coupling between the cavity modes and the baths described by the fields $\hat{g}(\omega)$, $\hat{b}(\omega)$, and $\hat{h}(\omega)$ at frequency ω, respectively; $G(\omega)$ is the coupling between the cavity mode $\hat{a}$ and the two-photon absorptive bath $\hat{S}$ with frequency ω; $\hat{S} = \hat{S}_{\text{in}}$ is for the couple in or $\hat{S} = \hat{S}_{\text{out}}$ for the couple out; and τ is the propagation time for light to travel from the source cavity to the target cavity.

We adapt the input-output theory. We now introduce the first Markov approximation, that the coupling constant is independent of frequency, that is,

$$
\begin{aligned}
\gamma_1(\omega) &= \sqrt{\kappa_{d1}/2\pi}, \quad \gamma_2(\omega) = \sqrt{\kappa_{d2}/2\pi}, \\
\gamma_3(\omega) &= \sqrt{\kappa_{e1}/2\pi}, \quad \gamma_4(\omega) = \sqrt{\kappa_{e2}/2\pi}, \\
G(\omega) &= \sqrt{\kappa_a^{\text{NL}}/2\pi}.
\end{aligned}
\tag{B2}
$$

Then the quantum Langevin equation for an arbitrary operator of the system $\hat{q}$ is derived as

$$
\begin{aligned}
\dot{\hat{q}} = & -i[\hat{q}, \hat{H}_{\text{sys}}] - [\hat{q}, \hat{d}^\dagger]\left\{\frac{\kappa_d}{2}\hat{d} + \sqrt{\kappa_{d1}}\hat{g}_{\text{in}}(t) + \sqrt{\kappa_{d2}}\hat{b}_{\text{in}}(t)\right\} \\
& + \left\{\frac{\kappa_d}{2}\hat{d}^\dagger + \sqrt{\kappa_{d1}}\hat{g}_{\text{in}}^\dagger(t) + \sqrt{\kappa_{d2}}\hat{b}_{\text{in}}^\dagger(t)\right\}[\hat{q}, \hat{d}] \\
& - [\hat{q}, \hat{a}^\dagger]\left\{\frac{\kappa_a}{2}\hat{a} + \sqrt{\kappa_{d2}\kappa_{e1}}\hat{d}(t-\tau) + \sqrt{\kappa_{e1}}\hat{b}_{\text{in}}(t-\tau)\right\} \\
& + \left\{\frac{\kappa_a}{2}\hat{a}^\dagger + \sqrt{\kappa_{d2}\kappa_{e1}}\hat{d}^\dagger(t-\tau) + \sqrt{\kappa_{e1}}\hat{b}_{\text{in}}^\dagger(t-\tau)\right\}[\hat{q}, \hat{a}] \\
& - \sqrt{\kappa_{e2}}[\hat{q}, \hat{a}^\dagger]\hat{h}_{\text{in}}(t) + \sqrt{\kappa_{e2}}\hat{h}_{\text{in}}^\dagger(t)[\hat{q}, \hat{a}] \\
& - [\hat{q}, \hat{a}^{\dagger 2}]\left\{\frac{\kappa_a^{\text{NL}}}{2}\hat{a}^2 + \sqrt{\kappa_a^{\text{NL}}}\hat{S}_{\text{in}}(t)\right\} \\
& + \left\{\frac{\kappa_a^{\text{NL}}}{2}\hat{a}^{\dagger 2} + \sqrt{\kappa_a^{\text{NL}}}\hat{S}_{\text{in}}^\dagger(t)\right\}[\hat{q}, \hat{a}^2],
\end{aligned}
\tag{B3}
$$

in which $\kappa_d = \kappa_{d1} + \kappa_{d2}$ and $\kappa_a = \kappa_{e1} + \kappa_{e2}$. The input-output relations for the cascaded system at the internally connected ports 2 and 3 are given by

$$
\hat{b}_{\text{out}}^{(2)}(t) = \hat{b}_{\text{in}}^{(2)}(t) + \sqrt{\kappa_{d2}}\hat{d}(t), \quad \hat{b}_{\text{in}}^{(3)}(t) = \hat{b}_{\text{out}}^{(2)}(t-\tau),
\tag{B4a}
$$

$$
\hat{b}_{\text{out}}^{(3)}(t) = \hat{b}_{\text{in}}^{(2)}(t-\tau) + \sqrt{\kappa_{d2}}\hat{d}(t-\tau) + \sqrt{\kappa_{e1}}\hat{a}(t). \tag{B4b}
$$

In the quantum cascaded model, we can neglect the propagation delay τ, setting $\tau \to 0$. Considering simultaneously that $\hat{b}_{\text{in}}(t)$ and $\hat{h}_{\text{in}}(t)$ are vacuum fluctuations and $\langle \hat{g}_{\text{in}} \rangle(t) = \alpha(t)$ for a coherent input, it follows that the cascaded quantum master equation for the density operator $\hat{\rho}(t)$ can be derived by setting $\langle \dot{\hat{q}}\hat{\rho} \rangle \equiv \langle \hat{q}\dot{\hat{\rho}} \rangle$. The master equation takes the form

$$
\begin{aligned}
\dot{\hat{\rho}} = & -i[\hat{H}_{\text{sys}}, \hat{\rho}] - \frac{\kappa_d}{2}[\hat{d}^\dagger, \hat{d}\hat{\rho}] + \frac{\kappa_d}{2}[\hat{d}, \hat{\rho}\hat{d}^\dagger] \\
& - \frac{\kappa_a}{2}[\hat{a}^\dagger, \hat{a}\hat{\rho}] + \frac{\kappa_a}{2}[\hat{a}, \hat{\rho}\hat{a}^\dagger] \\
& - \sqrt{\kappa_{d2}\kappa_{e1}}[\hat{a}^\dagger, \hat{d}\hat{\rho}] + \sqrt{\kappa_{d2}\kappa_{e1}}[\hat{a}, \hat{\rho}\hat{d}^\dagger] \\
& - \frac{\kappa_a^{\text{NL}}}{2}[\hat{a}^{\dagger 2}, \hat{a}^2\hat{\rho}] + \frac{\kappa_a^{\text{NL}}}{2}[\hat{a}^2, \hat{\rho}\hat{a}^{\dagger 2}] \\
& - \sqrt{\kappa_{d1}}[\alpha(t)\hat{d}^\dagger - \alpha^*(t)\hat{d}, \hat{\rho}],
\end{aligned}
\tag{B5}
$$

where the Lindblad operator in the third line accounts for the cascaded coupling, that is, the output from the source cavity can be connected to the input of the target cavity without there being a corresponding scattering from the target cavity back into the source cavity. In what follows we check the case that the target cavity decays only at the two ports to verify the validity of the numerical simulation of the quantum cascade method. We set $\kappa_{d1} = \kappa_{d2}$, $\kappa_{e1} = \kappa_{e2}$, and $\kappa_a^{\text{NL}} = 0$. Then we extract the Fock-state probabilities of the incident mode, reflected mode, and transmitted mode of the target cavity, respectively, where the reflected mode is defined as $\hat{c} = (\sqrt{\kappa_{d2}}\hat{d} + \sqrt{\kappa_{e1}}\hat{a})/\sqrt{\kappa_{d2} + \kappa_{e1}}$. The one-photon state for the incident mode is

$$
\begin{aligned}
|1_d\rangle\langle 1_d| = & |1_d 0_a\rangle\langle 1_d 0_a| + |1_d 1_a\rangle\langle 1_d 1_a| + \cdots \\
& + |1_d(N_a - 1)_a\rangle\langle 1_d(N_a - 1)_a| \\
= & |1\rangle_{dd}\langle 1| \otimes I_a,
\end{aligned}
\tag{B6}
$$
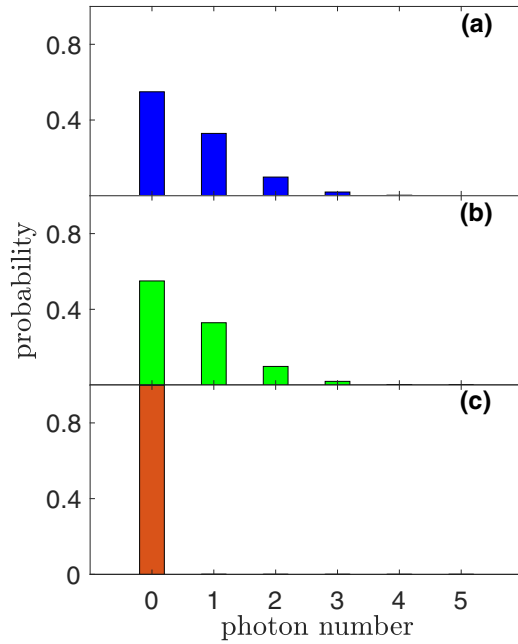
FIG. 13. Fock-state probabilities of (a) the incident mode $\hat{d}$, (b) the transmitted mode $\hat{a}$, and (c) the reflected mode $\hat{c}$ of the second cavity.

where N_a is the truncated dimension of the Hilbert space of the target cavity, $|1\rangle_d$ denotes the one-photon state in the source cavity's Hilbert space alone, and I_a is the identity matrix in the target cavity's Hilbert space. Then the probability of the one-photon state of the incident mode is given by

$$
\begin{aligned}
P_{1_d} &= \langle 1_d | \psi \rangle \langle \psi | 1_d \rangle \\
&= \mathrm{Tr}\{|1_d\rangle\langle 1_d|\hat{\rho}(t)\} \\
&= \mathrm{Tr}\{|1\rangle_{dd}\langle 1| \otimes I_a \hat{\rho}(t)\}.
\end{aligned} \tag{B7}
$$

We extract the Fock-state probabilities of the cavity mode $\hat{a}$ and reflected mode $\hat{c}$ in the same way. Figure 13 shows the Fock-state probabilities of the incident mode, intracavity mode (transmitted mode), and reflected mode of the target cavity. The Fock-state components of the incident mode satisfies the Poisson distribution with mean photon number $\bar{n} = 0.6$, and the photon-number distribution of the transmitted mode is almost the same as that of the incident mode, as shown in Figs. 13(a) and 13(b). Only the vacuum-state component in the incident field is reflected, as shown in Fig. 13(c). These results are consistent with the known conclusion, that is, the incident field will be totally transmitted when the decay rates of the cavity at the two ports are the same and the cavity has no intrinsic loss, which proves the validity of the numerical simulation of the quantum cascade method.

[1] M. Fleischhauer and M. D. Lukin, Quantum memory for photons: Dark-state polaritons, Phys. Rev. A **65**, 022314 (2002).

[2] M. Fleischhauer and M. D. Lukin, Dark-State Polaritons in Electromagnetically Induced Transparency, Phys. Rev. Lett. **84**, 5094 (2000).

[3] C. Liu, Z. Dutton, C. H. Behroozi, and L. V. Hau, Observation of coherent optical information storage in an atomic medium using halted light pulses, Nature (London) **409**, 490 (2001).

[4] D. F. Phillips, A. Fleischhauer, A. Mair, R. L. Walsworth, and M. D. Lukin, Storage of Light in Atomic Vapor, Phys. Rev. Lett. **86**, 783 (2001).

[5] J. I. Cirac, P. Zoller, H. J. Kimble, and H. Mabuchi, Quantum State Transfer and Entanglement Distribution among Distant Nodes in a Quantum Network, Phys. Rev. Lett. **78**, 3221 (1997).

[6] M. D. Eisaman, A. André, F. Massou, M. Fleischhauer, A. S. Zibrov, and M. D. Lukin, Electromagnetically induced transparency with tunable single-photon pulses, Nature (London) **438**, 837 (2005).

[7] C. H. van der Wal, M. D. Eisaman, A. André, R. L. Walsworth, D. F. Phillips, A. S. Zibrov, and M. D. Lukin, Atomic memory for correlated photon states, Science **301**, 196 (2003).

[8] K. M. Birnbaum, A. Boca, R. Miller, A. D. Boozer, T. E. Northup, and H. J. Kimble, Photon blockade in an optical cavity with one trapped atom, Nature (London) **436**, 87 (2005).

[9] B. Dayan, A. S. Parkins, T. Aoki, E. P. Ostby, K. J. Vahala, and H. J. Kimble, A photon turnstile dynamically regulated by one atom, Science **319**, 1062 (2008).

[10] P. Michler, A. Kiraz, C. Becher, W. V. Schoenfeld, P. M. Petroff, L. Zhang, E. Hu, and A. Imamoğlu, A quantum dot single-photon turnstile device, Science **290**, 2282 (2000).

[11] J. Tang, L. Tang, H. Wu, Y. Wu, H. Sun, H. Zhang, T. Li, Y. Lu, M. Xiao, and K. Xia, Towards On-Demand Heralded Single-Photon Sources via Photon Blockade, Phys. Rev. Appl. **15**, 064020 (2021).

[12] Q. A. Turchette, C. J. Hood, W. Lange, H. Mabuchi, and H. J. Kimble, Measurement of Conditional Phase Shifts for Quantum Logic, Phys. Rev. Lett. **75**, 4710 (1995).

[13] M. S. Zubairy, M. Kim, and M. O. Scully, Cavity-QED-based quantum phase gate, Phys. Rev. A **68**, 033820 (2003).

[14] B. Hacker, S. Welte, G. Rempe, and S. Ritter, A photon-photon quantum gate based on a single atom in an optical resonator, Nature (London) **536**, 193 (2016).

[15] A. Rauschenbeutel, G. Nogues, S. Osnaghi, P. Bertet, M. Brune, J. M. Raimond, and S. Haroche, Coherent Operation of a Tunable Quantum Phase Gate in Cavity QED, Phys. Rev. Lett. **83**, 5166 (1999).

[16] A. Reiserer, N. Kalb, G. Rempe, and S. Ritter, A quantum gate between a flying optical photon and a single trapped atom, Nature (London) **508**, 237 (2014).

[17] A. Biswas and G. S. Agarwal, Quantum logic gates using Stark-shifted Raman transitions in a cavity, Phys. Rev. A **69**, 062306 (2004).

[18] J. McKeever, A. Boca, A. D. Boozer, R. Miller, J. R. Buck, A. Kuzmich, and H. J. Kimble, Deterministic generation of single photons from one atom trapped in a cavity, Science **303**, 1992 (2004).

[19] B. Darquié, M. P. A. Jones, J. Dingjan, J. Beugnon, S. Bergamini, Y. Sortais, G. Messin, A. Browaeys, and P. Grangier, Controlled single-photon emission from a single trapped two-level atom, Science **309**, 454 (2005).

[20] A. Kuhn, M. Hennrich, and G. Rempe, Deterministic Single-Photon Source for Distributed Quantum Networking, Phys. Rev. Lett. **89**, 067901 (2002).

[21] R. Trivedi, M. Radulaski, K. A. Fischer, S. Fan, and J. Vučković, Photon Blockade in Weakly Driven Cavity Quantum Electrodynamics Systems with Many Emitters, Phys. Rev. Lett. **122**, 243602 (2019).

[22] H. Schmidt and A. Imamoğlu, Giant Kerr nonlinearities obtained by electromagnetically induced transparency, Opt. Lett. **21**, 1936 (1996).

[23] A. Imamoğlu, H. Schmidt, G. Woods, and M. Deutsch, Strongly Interacting Photons in a Nonlinear Cavity, Phys. Rev. Lett. **79**, 1467 (1997).

[24] S. Rebić, S. M. Tan, A. S. Parkins, and D. F. Walls, Large Kerr nonlinearity with a single atom, J. Opt. B **1**, 490 (1999).

[25] M. Fleischhauer, A. Imamoğlu, and J. P. Marangos, Electromagnetically induced transparency: Optics in coherent media, Rev. Mod. Phys. **77**, 633 (2005).

[26] P. D. Drummond and D. F. Walls, Quantum theory of optical bistability. I. Nonlinear polarisability model, J. Phys. A: Math. Gen. **13**, 725 (1980).

[27] N. Imoto, H. A. Haus, and Y. Yamamoto, Quantum nondemolition measurement of the photon number via the optical Kerr effect, Phys. Rev. A **32**, 2287 (1985).

[28] P. Grangier, J. A. Levenson, and J.-P. Poizat, Quantum nondemolition measurements in optics, Nature (London) **396**, 537 (1998).

[29] G. Nikoghosyan and M. Fleischhauer, Photon-Number Selective Group Delay in Cavity Induced Transparency, Phys. Rev. Lett. **105**, 013601 (2010).

[30] A. Reiserer, S. Ritter, and G. Rempe, Nondestructive detection of an optical photon, Science **342**, 1349 (2013).

[31] K. Xia, F. Nori, and M. Xiao, Cavity-Free Optical Isolators and Circulators Using a Chiral Cross-Kerr Nonlinearity, Phys. Rev. Lett. **121**, 203602 (2018).

[32] M.-X. Dong, K.-Y. Xia, W.-H. Zhang, Y.-C. Yu, Y.-H. Ye, E.-Z. Li, L. Zeng, D.-S. Ding, B.-S. Shi, G.-C. Guo, and F. Nori, All-optical reversible single-photon isolation at room temperature, Sci. Adv. **7**, eabe8924 (2021).

[33] W. Chen, M. Beck Kristin, R. Bücker, M. Gullans, D. Lukin Mikhail, H. Tanji-Suzuki, and V. Vuletić, All-optical switch and transistor gated by one stored photon, Science **341**, 768 (2013).

[34] T. Volz, A. Reinhard, M. Winger, A. Badolato, K. J. Hennessy, E. L. Hu, and A. Imamoğlu, Ultrafast all-optical switching by single photons, Nat. Photon. **6**, 605 (2012).

[35] D. E. Chang, A. S. Sørensen, E. A. Demler, and M. D. Lukin, A single-photon transistor using nanoscale surface plasmons, Nat. Phys. **3**, 807 (2007).

[36] M. Bajcsy, S. Hofferberth, V. Balic, T. Peyronel, M. Hafezi, A. S. Zibrov, V. Vuletic, and M. D. Lukin, Efficient All-Optical Switching Using Slow Light within a Hollow Fiber, Phys. Rev. Lett. **102**, 203902 (2009).

[37] I. Shomroni, S. Rosenblum, Y. Lovsky, O. Bechler, G. Guendelman, and B. Dayan, All-optical routing of single photons by a one-atom switch controlled by a single photon, Science **345**, 903 (2014).

[38] D. E. Chang, V. Vuletić, and M. D. Lukin, Quantum nonlinear optics—photon by photon, Nat. Photon. **8**, 685 (2014).

[39] O. Firstenberg, T. Peyronel, Q.-Y. Liang, A. V. Gorshkov, M. D. Lukin, and V. Vuletić, Attractive photons in a quantum nonlinear medium, Nature (London) **502**, 71 (2013).

[40] T. Peyronel, O. Firstenberg, Q.-Y. Liang, S. Hofferberth, A. V. Gorshkov, T. Pohl, M. D. Lukin, and V. Vuletić, Quantum nonlinear optics with single photons enabled by strongly interacting atoms, Nature (London) **488**, 57 (2012).

[41] A. Faraon, I. Fushman, D. Englund, N. Stoltz, P. Petroff, and J. Vučković, Coherent generation of non-classical light on a chip via photon-induced tunnelling and blockade, Nat. Phys. **4**, 859 (2008).

[42] I. Fushman, D. Englund, A. Faraon, N. Stoltz, P. Petroff, and J. Vučković, Controlled phase shifts with a single quantum dot, Science **320**, 769 (2008).

[43] S. E. Harris and L. V. Hau, Nonlinear Optics at Low Light Levels, Phys. Rev. Lett. **82**, 4611 (1999).

[44] H. Kang and Y. Zhu, Observation of Large Kerr Nonlinearity at Low Light Intensities, Phys. Rev. Lett. **91**, 093601 (2003).

[45] C. Hamsen, K. N. Tolazzi, T. Wilk, and G. Rempe, Strong coupling between photons of two light fields mediated by one atom, Nat. Phys. **14**, 885 (2018).

[46] H.-Y. Lo, Y.-C. Chen, P.-C. Su, H.-C. Chen, J.-X. Chen, Y.-C. Chen, I. A. Yu, and Y.-F. Chen, Electromagnetically-induced-transparency-based cross-phase-modulation at attojoule levels, Phys. Rev. A **83**, 041804(R) (2011).

[47] X. Yang, K. Ying, Y. Niu, and S. Gong, Reversible self-Kerr nonlinearity in an N-type atomic system through a switching field, J. Opt. **17**, 045505 (2015).

[48] M. J. Werner and A. Imamoğlu, Photon-photon interactions in cavity electromagnetically induced transparency, Phys. Rev. A **61**, 011801(R) (1999).

[49] S. Rebić, A. S. Parkins, and S. M. Tan, Photon statistics of a single-atom intracavity system involving electromagnetically induced transparency, Phys. Rev. A **65**, 063804 (2002).

[50] H. D. Simaan and R. Loudon, Quantum statistics of single-beam two-photon absorption, J. Phys. A: Math. Gen. **8**, 539 (1975).

[51] H. D. Simaan and R. Loudon, Off-diagonal density matrix for single-beam two-photon absorbed light, J. Phys. A: Math. Gen. **11**, 435 (1978).

[52] N. Bartolo, F. Minganti, W. Casteels, and C. Ciuti, Exact steady state of a Kerr resonator with one- and two-photon driving and dissipation: Controllable Wigner-function multimodality and dissipative phase transitions, Phys. Rev. A **94**, 033841 (2016).

[53] F. Minganti, N. Bartolo, J. Lolli, W. Casteels, and C. Ciuti, Exact results for Schrödinger cats in driven-dissipative systems and their feedback control, Sci. Rep. **6**, 26987 (2016).

[54] T. Li, Z. Gao, and K. Xia, Nonlinear-dissipation-induced nonreciprocal exceptional points, Opt. Express **29**, 17613 (2021).

[55] M. S. Zubairy and J. J. Yeh, Photon statistics in multiphoton absorption and emission processes, Phys. Rev. A **21**, 1624 (1980).

[56] H. Paul, U. Mohr, and W. Brunner, Change of photon statistics due to multi-photon absorption, Opt. Commun. **17**, 145 (1976).

[57] L. Gilles and P. L. Knight, Two-photon absorption and nonclassical states of light, Phys. Rev. A **48**, 1582 (1993).

[58] K. M. Gheri, W. Alge, and P. Grangier, Quantum analysis of the photonic blockade mechanism, Phys. Rev. A **60**, R2673 (1999).

[59] J. Sheng, X. Yang, H. Wu, and M. Xiao, Modified self-kerr-nonlinearity in a four-level N-type atomic system, Phys. Rev. A **84**, 053820 (2011).

[60] M. Afzelius and C. Simon, Impedance-matched cavity quantum memory, Phys. Rev. A **82**, 022310 (2010).

[61] J. Dilley, P. Nisbet-Jones, B. W. Shore, and A. Kuhn, Single-photon absorption in coupled atom-cavity systems, Phys. Rev. A **85**, 023834 (2012).

[62] J. H. Chow, I. C. M. Littler, D. S. Rabeling, D. E. McClelland, and M. B. Gray, Using active resonator impedance matching for shot-noise limited, cavity enhanced amplitude modulated laser absorption spectroscopy, Opt. Express **16**, 7726 (2008).

[63] A. E. Siegman, *Lasers* (University Science Books, Sausalito, 1986).

[64] H. J. Carmichael, Quantum Trajectory Theory for Cascaded Open Systems, Phys. Rev. Lett. **70**, 2273 (1993).

[65] C. W. Gardiner, Driving a Quantum System with the Output Field from Another Driven Quantum System, Phys. Rev. Lett. **70**, 2269 (1993).

[66] C. W. Gardiner and A. S. Parkins, Driving atoms with light of arbitrary statistics, Phys. Rev. A **50**, 1792 (1994).